

See discussions, stats, and author profiles for this publication at: <https://www.researchgate.net/publication/229898851>

Theoretical analysis of the resonance CARS spectra of diacetylene single crystals

ARTICLE *in* JOURNAL OF RAMAN SPECTROSCOPY · NOVEMBER 1992

Impact Factor: 2.67 · DOI: 10.1002/jrs.1250231104

CITATIONS

6

READS

18

2 AUTHORS:



Arnulf Materny

Jacobs University

198 PUBLICATIONS **2,336** CITATIONS

SEE PROFILE



Wolfgang Kiefer

University of Wuerzburg

881 PUBLICATIONS **9,877** CITATIONS

SEE PROFILE

Theoretical analysis of the resonance Raman spectra of diacetylene single crystals

A. Materny and W. Kiefer

Citation: *J. Chem. Phys.* **97**, 841 (1992); doi: 10.1063/1.463187

View online: <http://dx.doi.org/10.1063/1.463187>

View Table of Contents: <http://jcp.aip.org/resource/1/JCPSA6/v97/i2>

Published by the AIP Publishing LLC.

Additional information on J. Chem. Phys.

Journal Homepage: <http://jcp.aip.org/>


Journal Information: http://jcp.aip.org/about/about_the_journal

Top downloads: http://jcp.aip.org/features/most_downloaded

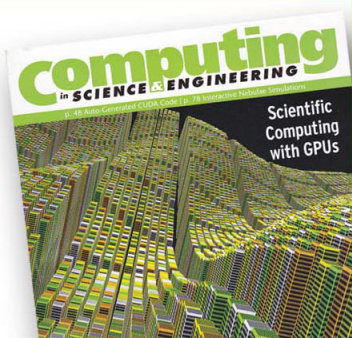
Information for Authors: <http://jcp.aip.org/authors>

ADVERTISEMENT

**SHARPEN YOUR
COMPUTATIONAL
SKILLS.**



Subscribe for
\$49 | year



computing
in **SCIENCE & ENGINEERING**

Scientific
Computing
with GPUs

Theoretical analysis of the resonance Raman spectra of diacetylene single crystals

A. Materny and W. Kiefer^{a)}

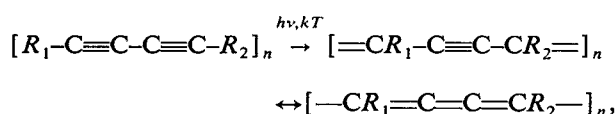
Institut für Physikalische Chemie der Universität Würzburg, Marcusstraße 9-11, W-8700 Würzburg, Germany

(Received 5 February 1992; accepted 30 March 1992)

Resonance Raman spectra of polymer chains in the single crystals of the diacetylenes FBS (2,4-hexadiynylene-di-p-fluorobenzene sulfonate), TS/FBS [6-(p-toluene sulfonyl oxy)-2,4-p-fluorobenzene sulfonate] and TS6 (2,4-hexadiynylene-di-p-toluene sulfonate) are described theoretically by means of a Franck–Condon model, which considers a chain length dependence. The electronic transition energies and matrix elements are calculated by means of a linear-combination-of-atomic-orbitals–molecular-orbital method calculation in the Hückel approach. We are able to describe the Raman excitation profiles as well as the Raman band profiles for two Raman active modes, i.e., the C=C-, and the C≡C-stretching vibrations of the polymer chains. The model also contains a description of a side group vibrational mode which is enhanced by Fermi resonance with the C=C-stretching vibration. Observed Raman excitation profiles can be well simulated by these calculations. An evaluation of the parameters shows a strong influence of defects, which is described by including inhomogeneous broadening in the theoretical model. An interaction between ensemble and intramolecular properties due to defects can be shown. Simulation of the Raman band profiles yields information on the influence of chain length distribution. Changes of position and Raman band profile as well as of the strength of the Fermi resonance can be explained by the enhancement of modes belonging to polymer chains having different chain lengths. A considerable influence of the substituents results in remarkable changes of several parameters on which the model calculation is based.

I. INTRODUCTION

Crystalline polydiacetylenes (PDAs) exhibit very large values for the third-order susceptibility $\chi^{(3)}$. These are comparable to those of inorganic semiconductors.¹ PDAs are also available as Langmuir–Blodgett layers² or solutions,³ which show similar large values of $\chi^{(3)}$. Therefore, they are attractive candidate materials for nonlinear optical signal processing applications. The optical properties of PDAs are attributed to the fully conjugated backbone structure, which arises from the solid-state polymerization of the diacetylene monomers (DAs). The DAs undergo the following topochemical reaction



when treated with high energy radiation or heat. There exist two mesomeric structures of the polymer backbone, an acetylenic and a butatrienic one. In most PDAs the acetylenic form is the preferred one. Since the discovery by Wegner⁴ a great variety of DAs with different substituents R_1 and R_2 could be synthesized. The forms of the side groups strongly influence the properties of the DAs and PDAs. Particular properties of these polymers are the reversible and irreversible color changes of various kinds.^{5,6} These chromisms most probably are due to changes of the backbone structure of the PDA chains induced by side group distortions. Therefore, a good knowledge about the structure of the chains is the supposition for an understanding of nonlinear as well as chromatic effects.

Different forms of experimental methods were applied to investigate the electronic and vibronic properties of PDA chains. Especially optical spectroscopy proved to be a valuable tool in this context. The DAs do not show any absorption in the visible, while the absorption spectra of the PDA chains nearly cover the whole visible spectral region.⁷ This absorption is due to an $^1A_g \rightarrow ^1B_u$ transition for the π -electron system of the PDA backbone with excitonic character.⁸ Raman spectra of PDAs therefore normally are obtained under resonance conditions. Until now several researchers^{9–11} performed investigations of the vibrational modes of PDA chains by means of resonance Raman spectroscopy. The resonance with the absorption of the conjugated π -electron system gives rise to only a few Raman lines above 500 cm^{-1} which all belong to symmetric A_g modes of the PDA backbone.¹² In the wave number region from $500\text{--}3500\text{ cm}^{-1}$ only four prominent Raman lines, labeled ν_1 to ν_4 , and about six combination frequencies can be observed.¹³

Until now only a few theoretical approaches have been made in order to explain the resonance Raman spectra of PDA chains. Recently, we have performed comprehensive experimental studies in various DAs by means of one-photon (absorption, fluorescence),^{6,14} two-photon (resonance Raman),^{14,15} and four-photon (resonance coherent anti-Stokes Raman scattering, CARS)¹⁴ spectroscopy. For the explanation of these experimental results we developed a theoretical model which is capable of describing these spectra,^{16,17} and also for crystals showing chromism effects. The experimental and theoretical studies were undertaken on three different DAs. The first one is the mostly investigated DA TS6¹⁸ (2,4-hexadiynylene-di-p-toluene sulfonate) with the substituents $R_1=R_2: -CH_2-O-SO_2-\oplus-CH_3$. The oth-

^{a)} Author to whom correspondence should be addressed.

ers are FBS¹⁹ (2,4-hexadiynylene-di-p-fluorobenzene sulfonate) with $R_1 = R_2$: $-\text{CH}_2-\text{O}-\text{SO}_2-\text{O}-\text{F}$, and TS/FBS^{20,21} with $R_1 \equiv \text{TS6}$ and $R_2 \equiv \text{FBS}$. All three DAs crystallize as single crystals with a monoclinic lattice. After growing, these crystals exhibit a slight reddish color, which is due to a small amount (less than 1%) of polymer chains arising during the crystal growth. These PDA chains are distributed over the whole crystal bulk, embedded in a matrix of DA molecules. All polymer chains are parallel to the b axis of the crystal lattice, which leads to a high anisotropy of most optical properties of these DA crystals. In this state optimal conditions are given for an investigation of the properties of the polymer backbones. Measurements^{6,14} of absorption, resonance Raman, and resonance CARS spectra showed that only relatively short (< 20 monomer units) PDA chains exist in these DA crystals. Therefore, we developed a theoretical model which considers a distribution of chain lengths. This model already was applied to absorption spectra with great success.¹⁷ A theoretical approach to resonance Raman spectra of TS6 PDAs were performed by Batchelder and Bloor¹³ several years ago. Because of the much greater chain lengths in the PDA crystals they did not consider a chain length distribution. However, for DA crystals such an approximation would yield no satisfactory results. In this paper we show how the model used already for the description of absorption spectra¹⁷ can be extended to describe resonance Raman spectra of the DA crystals mentioned above. Preliminary results on TS/FBS single crystals have already been published.¹⁶

Here we present the theory needed for the calculation of resonance Raman spectra in DAs. Based on the theory for absorption and making use of several additional assumptions, which are described in Sec. II, we give in Sec. III the results of our calculations and compare them with the measured resonance Raman spectra of the three DAs. A discussion of the results is also included in this section. Experimental details concerning the crystal growth of the symmetrically substituted DAs TS6 and FBS and of the unsymmetrically substituted TS/FBS are given in Refs. 18 and 20, respectively. For the measurements of the resonance Raman spectra a backscattering arrangement has been used and the Raman signals were detected applying a multichannel detection system. Measurements could be performed for variable temperatures. In all experiments the polarizations of incident and scattered light were chosen to be parallel to the chain direction. For further details see Ref. 15.

II. BASIC THEORY

In this section we present the theoretical model developed for the calculation of the resonance Raman (RR) spectra of DAs. RR scattering is basically described by the well-known Kramers–Heisenberg–Dirac equation,²² which arises from second order perturbation theory. At first we consider scattering from a single chain with definite length. The intensity of the scattered light with wave number $\tilde{\nu}_f$ for excitation with irradiance I_0 at wave number $\tilde{\nu}_0$ is given by²³

$$I_{f-i} = \frac{\pi^2}{\epsilon_0^2} I_0 (\tilde{\nu}_0 \pm \tilde{\nu}_f)^4 \sum_{\rho, \sigma} (\alpha_{\rho\sigma})_{fi} (\alpha_{\rho\sigma})_{fi}^*, \quad (1)$$

where ϵ_0 is the permittivity of free space. $(\alpha)_{fi}$ is the polarizability tensor for transition $f \leftarrow i$, ρ and σ are the polarization indices for scattered and incident light, respectively. In the following we assume all polarizations to be parallel to the chain direction, which is taken as x axis of the system. i and f label the initial and the final state, respectively. The quantum mechanical expression for the xx th element of the transition polarizability is given by²²

$$(\alpha_{xx})_{fi} = \frac{\hbar e^2}{8\pi^3 c^3 m_e^2 \tilde{\nu}_f^2} \times \sum_r \left(\frac{[\hat{H}'_x]_{fr} [\hat{H}'_x]_{ri}}{\tilde{\nu}_{ri} - \tilde{\nu}_0 + i\Gamma_r} + \frac{[\hat{H}'_x]_{fr} [\hat{H}'_x]_{ri}}{\tilde{\nu}_{ri} + \tilde{\nu}_0 + i\Gamma_r} \right), \quad (2)$$

where r labels all states of the unperturbed system. m_e is the electron mass, and \hat{H}'_x is the x th component of the Hamiltonian of the perturbation of the system. Applying the dipole approximation and neglecting the nonresonant term in Eq. (2), one obtains the usual expression for the polarizability²⁴

$$(\alpha_{xx})_{fi} = \frac{1}{\hbar c} \sum_r \frac{[\mu_x]_{fr} [\mu_x]_{ri}}{\tilde{\nu}_{ri} - \tilde{\nu}_0 + i\Gamma_r}, \quad (3)$$

where μ is the appropriate dipole matrix element. The SI units of the different expressions are I : W, I_0 : W m^{-2} , $(\alpha_{xx})_{fi}$: $\text{C V}^{-1} \text{ m}^2$, and $[\mu_x]_{fr}$: C m. In the case where cm^{-1} is used as unit for wave numbers, the right sides of Eqs. (2) and (3) have to be multiplied by a factor 10^8 .

Assuming that the states $|i\rangle$, $|r\rangle$, and $|f\rangle$ are adiabatic Born–Oppenheimer states, we can split them into electronic and vibrational states

$$\begin{aligned} |i\rangle &= |g\rangle |m\rangle, \\ |r\rangle &= |e\rangle |v\rangle, \\ |f\rangle &= |g\rangle |n\rangle. \end{aligned}$$

Here, $|g\rangle$ and $|e\rangle$ are the electronic ground and excited state, respectively. $|m\rangle$ and $|n\rangle$ are the vibrational states belonging to the initial and final states, respectively, and $|v\rangle$ is the intermediate vibrational state. Applying the crude Born–Oppenheimer approximation, we can separate the dipole matrix elements in Eq. (3) according to²⁵

$$[\mu_x]_{fr} = \langle n | [\mu_x]_{ge}^0 | v \rangle = [\mu_x]_{ge}^0 \langle n | v \rangle, \quad (4)$$

where $[\mu_x]_{ge}^0$ is the electronic equilibrium transition moment taken at equilibrium of the nuclei, and $\langle n | v \rangle$ is a Franck–Condon (F–C) integral. Since the resonance Raman spectra were taken only at very low temperatures, it is not necessary to consider other states for $|m\rangle$ than $|0\rangle$. As mentioned above, there exist only few intense Raman lines for PDA as well as for DA crystals.

Calculations of the resonance Raman spectra were performed for the four most prominent chain modes, as mentioned above. The ν_1 mode at $\sim 2050 \text{ cm}^{-1}$ involves considerable stretching of the triple bond and $\nu_2 \sim 1480 \text{ cm}^{-1}$ the stretching of the double bond. Modes ν_3 at $\sim 1200 \text{ cm}^{-1}$ and ν_4 at $\sim 950 \text{ cm}^{-1}$ describe rotations with the C=C and C≡C bonds as axis.²⁶ Mode ν_3 involves considerable stretching of the single bond, while in mode ν_4 side group motions are included.²⁷ Batchelder and Bloor¹³ have mea-

sured the phonon frequencies of both, the ground and excited state fundamental modes, and have found that they differ by less than 5% in all cases. Measurements on TS/FBS DA crystals support these results.⁶ Resonance Raman spectra exhibit several combination modes. The frequencies observed in these investigations^{1,12} show that a harmonic approximation of the potential functions for ground and excited electronic states is justified. This helps us to find a relatively simple relation for the F–C integrals. The vibrational overlap integrals are computed applying the recurrence relations of Manneback.²⁸ The F–C integrals are zero if ground and excited state wave functions are orthogonal. This is not true if the curvatures and/or the equilibrium positions of the appertaining potentials differ. Since the phonon frequencies of ground and excited state are similar, as mentioned above, we neglect the differences in the curvature of the potentials. The observation of progressions of the different harmonics supports the assumption that mainly the equilibrium positions of the ground and excited state potentials q_k^0 and q_k^e are relatively shifted against one another,²⁹ for the different modes k . These shifts are called Δq_k . In the following we only consider final states which belong to fundamentals of single vibrational modes k . Applying a separation according to Eq. (4) to the expression in Eq. (3) we result in a product of two F–C integrals, which can be computed as follows:

$$\langle 1, |v\rangle \langle v| 0\rangle = \left(\prod_{k=1}^4 \frac{a_k^{2v_k}}{2^{v_k} v_k!} \exp(-a_k^2/2) \right) \times \left(\frac{a_s^2 - 2v_s}{\sqrt{2} a_s} \right), \quad (5)$$

where the product is taken over the four vibrational modes v_1 to v_4 , described by the quantum numbers v_k and the dimensionless F–C vibrational shift parameter (FCSP) a_k . a_k is related to the change in bond length Δr_k , which in a simple chain model is proportional to the normal coordinate shift Δq_k . This relation is given by³⁰

$$a_k = \left(\frac{\pi m_c c}{\hbar} N_k^0 \tilde{\nu}_k \right)^{1/2} \Delta r_k, \quad (6)$$

where N_k^0 is the number of bonds concerned with mode k . $\tilde{\nu}_k$ is the vibrational fundamental wave number of mode k . m_c is the mass of a carbon atom. We want to mention that the definition of the FCSPs a_k as given in Eq. (6) differs by a factor $1/\sqrt{2}$ from that given in some other presentations.^{28,29} The expressions given above are all valid for single chains only with a distinct chain length. In the following, we consider a more realistic model for the DA crystals with a distribution of chain lengths. As mentioned above, the lengths of the polymer chains in DA crystals are less than 20 monomer units. Chains of this length show discernible electronic and vibronic properties. Therefore, the physical properties have to be treated not as constants, but as functions of chain length n . Investigations of the absorption of oligomer chains in the DA crystals TS6³¹, FBS³², and TS/FBS⁶ give in principle the relation between absorption energy and chain length. However, we were not able to find sufficient information for all required chain length dependencies. But, many

investigations have been made in this connection on polyenes,³³ especially on carotenoids³⁴ and mostly on polyacetylenes.^{35–37} For many optical properties a great analogy between polyenes and PDAs was found.³⁸ Therefore, we transferred relations found for polyenes on to PDAs. For the description of the distribution of chain lengths we use a log-normal distribution function which mostly resembles the asymmetric form found for PDAs.³⁹ This function is given by

$$P(n) = \frac{1}{\sqrt{\pi n \Delta}} \exp \left[-\frac{\ln^2(n/n_0)}{\Delta^2} \right], \quad (7)$$

where Δ characterizes the width of the distribution. n is the number of monomer units and n_0 is the peak value. Such distributions also yielded good results for modeling chain length distributions in polyacetylenes.³⁵ The fraction of polymer chains with a particular length n is given by $P'(n) = n \cdot P(n)$.

As mentioned above, the absorption in PDAs is of excitonic character. However, in many later works it was proved that a model using electronic band structures consisting of valence and conduction band^{40,41} is a very good approximation for a description of the optical properties of PDAs in many cases. In our work we use a linear-combination-of-atomic-orbitals (LCAO) molecular orbital method in the Hückel approach (HMO). For a more detailed description we refer to Ref. 17. It proved to be sufficient only to consider highest occupied molecular orbital–lowest unoccupied molecular orbital (HOMO–LUMO) transitions. For the transition energy we used a relation, which is based on a transition from the HMO to a tight-binding approach,⁴²

$$\Delta E_{1,1} = 2 \left(\beta_1^2 + \beta_2^2 + 2\beta_1\beta_2 \cos \left[\frac{2n\pi}{2n+c} \right] \right)^{1/2}. \quad (8)$$

β_1 and β_2 are the interaction energies between two adjacent p - π orbitals (resonance integrals) for the different bondings. c is a factor which corrects the theoretical expression in Eq. (8) for chains with a finite length. Measured chain length dependent absorption energies are preferable to the numerical calculated energy values. Therefore, we estimated the parameters in Eq. (8) by an adjustment to the measured energies. In Table I we compile the computed parameters.¹⁷ The corresponding electronic transition moment is given by

$$[\mu_x]_{1,1}^0 = \sum_{r,s=1}^{4n} a_{1,r} a_{1,s} \langle \varphi_r | X | \varphi_s \rangle, \quad (9)$$

where the coefficients $a_{1,r}$ and $a_{1,s}$ can be obtained by solving the Hückel secular equations. $|\varphi\rangle$ are Slater-type atomic or-

TABLE I. Parameters obtained for a fit of $\Delta E_{1,1}$ [see Eq. (8)] to the absorption energies of stable oligomer chains for the considered DA crystals.^a β_1 and β_2 are the resonance integrals for the different bondings. c is a correction factor. Absorption energies were taken from the references given in the table.

DA crystal	β_1 [cm ⁻¹]	β_2 [cm ⁻¹]	c	(Ref.)
TS6	– 21 603	– 29 528	1	(45)
FBS	– 20 332	– 28 223	1	(32)
TS/FBS	– 21 062	– 29 001	1	(6)

^a Data taken from Ref. 17.

bitals with the standard carbon exponent⁴³ $\zeta = 1.6250$. $4n$ is the number of carbon atoms, which build up the polymer backbone.

An observation of the Raman spectral changes during the solid-state polymerization of DAs by Melveger *et al.*⁴⁴ shows that the Raman frequencies are lowered, when chains become longer. Same observation can be made for the vibronic frequencies of oligomer chains in DA crystals.⁴⁵ Because we do have no knowledge of the exact chain length dependence, we have to estimate it from the fits to the measured Raman spectra. Due to the great analogy to polyacetylene we take the following expression⁴⁶ for the wave number position of mode k :

$$\tilde{\nu}_k(n) = \tilde{\nu}_k^\alpha + \tilde{\nu}_k^\beta/n. \quad (10)$$

The FCSPs a_k were already estimated from calculations of the absorption spectra of DAs.¹⁷ They were found to be independent of chain length. Their values are listed in Table II for the modes ν_1 to ν_4 . As mentioned above, only these four modes and their combinations are taken into consideration for the calculations. There is one more strong line in the resonance Raman spectra of TS6, FBS, and TS/FBS next to the ν_2 line. This line can be assigned to a CH_2 -scissors vibration of the side groups, which is enhanced by a Fermi resonance with the ν_2 mode.⁴⁷ A theoretical treatment of this resonance enhancement is given for example in Ref. 48. It results in the following ratio of the products of the transition matrix elements [see Eq. (3)]:

$$\frac{([\mu_x]_{fr}[\mu_x]_{ri})_{\text{CH}_2}}{([\mu_x]_{fr}[\mu_x]_{ri})_2} = \left(\frac{(4|W_{\text{CH}_2,2}|^2 + \delta^2)^{1/2} - \delta}{4|W_{\text{CH}_2,2}|^2 + \delta^2 + \delta} \right)^{1/2}, \quad (11)$$

where $W_{\text{CH}_2,2}$ is the matrix element of the perturbation function W and δ is the energy separation of the unperturbed levels. The wave number position of the perturbed CH_2 vibration is related to the one of ν_2 by

$$\tilde{\nu}_{\text{CH}_2} = \tilde{\nu}_2 - (4|W_{\text{CH}_2,2}|^2 + \delta^2)^{1/2}. \quad (12)$$

For the estimation of the chain length dependence of the two parameters $W_{\text{CH}_2,2}$ and δ we use results reported in Ref. 47, where the strain dependence of the vibrational modes of DA crystals was investigated. In these works the strain dependence of the two Fermi parameters was shown to be qualitatively the same as that of the frequencies of the modes. Assuming that the change of π -electron density due to strain or compression is comparable to changes which arise from different chain lengths, we result in

$$W_{\text{CH}_2,2}(n) = W_{\text{CH}_2,2}^\alpha + W_{\text{CH}_2,2}^\beta/n, \quad (13a)$$

and

$$\delta(n) = \delta^\alpha + \delta^\beta/n. \quad (13b)$$

This confirms the observation that many electronic properties of DA oligomer chains vary with conjugation length, usually with a length⁻¹ dependence.³ Because the estimated widths of the chain length distributions are small for DA crystals¹⁷ small deviations from the assumed n dependencies would be of no consequence. The values of the parameters in Eqs. (13a) and (13b) are estimated from the fits to the measured resonance Raman spectra.

The calculations of the absorption spectra of the DA crystals¹⁷ yielded an interesting result. The widths of the absorption lines were strongly influenced by crystal quality. A broadening of the lines due to defects ("inhomogeneous" broadening) could be observed which did not depend on the length of the polymer chains. In contrast to this the part of the broadening, which depends on n , was found to be constant for each type of DAs ("homogeneous" broadening). The parameter Γ describing the linewidths was replaced by Σ which was the sum of the homogeneous and inhomogeneous linewidth, which could not be totally separated in absorption theory. The influence of inhomogeneous broadening due to variations in the interaction between molecules and the solvent on resonance Raman excitation profiles was estimated by Siebrand *et al.*⁴⁹ The defects are assumed to shift the electronic energies of the system, which results in a distribution of energies. We assume the values of the electronic transition wave numbers ($\tilde{\nu}_{eg}$) to have a Lorentzian distribution $\mathcal{L}(\tilde{\nu}_{eg})$ around a mean value $\langle \tilde{\nu}_{eg} \rangle$ with width γ ,

$$\mathcal{L}(\tilde{\nu}_{eg}) = \frac{\gamma/\pi}{(\tilde{\nu}_{eg} - \langle \tilde{\nu}_{eg} \rangle)^2 + \gamma^2}. \quad (14)$$

The expression for the Raman intensity in Eq. (1) is now multiplied by the Lorentzian and then integrated over all $\tilde{\nu}_{eg}$. The integral can be evaluated analytically, either by partial fractions or by contour integration. The final expression is given below by Eq. (18b). The inhomogeneous width γ does not depend on the chain length, while for the homogeneous width Γ a chain length dependence as reported in Ref. 17 is taken

$$\Gamma = \Gamma^\alpha + \Gamma^\beta/n^2. \quad (15)$$

The values of Γ^β are taken from Ref. 17 (see Table II). Γ^α and γ are estimated from a fit to the measured resonance Raman spectra. For simplicity we assume the homogeneous as well as the inhomogeneous broadening to be the same for all considered states.

Besides to resonance Raman excitation profiles we also calculated Raman line profiles for different excitation wavelengths applying a Lorentzian distribution function $L(\tilde{\nu}, \tilde{\nu}_k, n)$, which describes the broadening of the Raman levels for each mode position $\tilde{\nu}_k$,

TABLE II. Mean values of the least-squares fit of the theoretical absorption function to P -absorption spectra of the considered DA crystals.^a The variations of the F-C shift parameters a_k were less than 10%, those for the chain length dependent damping Γ^β less than 5%. Values for DA TS6 are given for the two phases (*B* and *A*) existing at low temperatures. The last row contains values for Γ^β estimated for TS6 PDA crystals at $T = 295 \text{ K}$ ^b [TS6 (*RT*)].

DA crystal	a_1	a_2	a_3	a_4	$\Gamma^\beta [\text{cm}^{-1}]$
FBS	0.70	0.96	0.74	0.37	8100
TS/FBS	0.80	0.87	0.55	0.85	7500
TS6 (<i>B</i>)	0.71	0.95	0.38	0.93	6200
TS6 (<i>A</i>)	0.38	0.59	0.54	0.79	4500
TS6 (<i>RT</i>)	0.57	0.78	0.30	0.44	...

^a See Ref. 17.

^b Data taken from Ref. 13.

$$L(\tilde{\nu}, \tilde{\nu}_k, n) = \frac{\sigma/\pi}{(\tilde{\nu} - \tilde{\nu}_k)^2 + \sigma^2}, \quad (16)$$

where $\tilde{\nu}$ is the observed wave number position. For the line width σ the same form of dependence of the length of polymer chains is assumed as for the homogeneous broadening in Eq. (15)

$$\sigma(n) = \sigma^\alpha + \sigma^\beta/n^2. \quad (17)$$

The final expression for the total intensity of the fundamen-

tal mode k can now be written as

$$I_{1_g, 1_g, 0}(\tilde{\nu}, \tilde{\nu}_0, n) = K \sum_n L(\tilde{\nu}, \tilde{\nu}_k, n) P'(n) ([\mu_x]_{1_g, 1_g}^0)^4 \cdot \sum_v \sum_{v'} \langle 1_k | v \rangle \langle v | 0 \rangle \times \langle 1_k | v' \rangle \langle v' | 0 \rangle \cdot R(\tilde{\nu}_0, \tilde{\nu}_{1_g, 0, 1_g, v}, n), \quad (18a)$$

where

$$R(\tilde{\nu}_0, \tilde{\nu}_{1_g, 0, 1_g, v}, n) = \frac{(\epsilon_v \epsilon_v - \Sigma^2)(\epsilon_v - \epsilon_v)^2 + 2\Gamma \Sigma((\epsilon_v^2 + \Sigma^2) + (\epsilon_v^2 + \Sigma^2))}{(\epsilon_v^2 + \Sigma^2)(\epsilon_v^2 + \Sigma^2)((\epsilon_v - \epsilon_v)^2 + 4\Gamma^2)} \quad (18b)$$

is the resonance part and K contains all constant terms. The quantum numbers 1_g and 1_g label the electronic states in the HMO notation (see above), while the other quantum numbers label the vibrational states. $\Sigma = \Gamma + \gamma$, is the sum of the homogeneous and the inhomogeneous broadening. $\epsilon_v = \tilde{\nu}_{1_g, 0, 1_g, v} - \tilde{\nu}_0$, is the difference between the wave numbers of the intermediate state and of the excitation energy.

III. RESULTS AND DISCUSSION

In this section we apply the theoretical model derived in Sec. II to the simulation of resonance Raman spectra and calculations of Raman excitation profiles for FBS, TS/FBS, and TS6 DA crystals. Calculations for several series of resonance Raman spectra were taken for each type of DAs. The parameters listed in Tables I and II were used as constant quantities. They were estimated as mean values of those derived from calculations of the absorption spectra of the different DA crystals. From absorption spectra only the parameters Δ and n_0 , which give the width and center of the distribution of chain lengths, respectively, were taken for the calculations related to Raman scattering. The other parameters were estimated by an iterative fitting of the Raman excitation profile (REP) and of the series of Raman line profiles (RLP) obtained for each crystal. We restricted our calculations to the spectral regions around the ν_1 (C \equiv C stretching) and ν_2/ν_{CH_2} (C=C stretching and Fermi resonance enhanced CH₂ bending) vibrations. The modes ν_3 and ν_4 were included in the summation over the intermediate states. For simplicity their wave numbers $\tilde{\nu}_3$ and $\tilde{\nu}_4$ were assumed to be independent on the chain length n . The mean positions in the Raman spectra, obtained for different excitation energies, were taken for this purpose. The summation over the intermediate states was performed up to combination and harmonic vibrations of second order. All experimental spectra were corrected for absorption, laser intensity and for the $(\tilde{\nu}_0 - \tilde{\nu}_i)^4$ law. If not stated otherwise, all parameters given in this work are for $T = 10$ K. The fits were performed by means of a Levenberg–Marquardt method.⁵⁰ It uses components of the Hessian matrix to give information about the curvature of the basis function with respect to their parameters. This nonlinear least-squares routine is good for solving also problems with difficult parameter de-

pendencies. The fit program gives the possibility to fix distinct parameters and further to give weighting values for each adjusted point of the curve.

Firstly we discuss results obtained for the REP calculation. The parameters which mainly influence the form of the calculated REPs are the FCSPs and the damping parameters γ and Γ . As stated above the values for the FCSPs as well as for Γ^β were estimated from computations of absorption spectra. We found these values to be of sufficient use for the Raman calculations. Variations of these parameters did not remarkably improve the calculated REPs, confirming the applied model. The calculation of REPs for FBS and TS/FBS DA crystals yielded similar results. In all cases we achieved good agreement between experiment and theory. Figures 1 and 2 show examples obtained for an FBS and a TS/FBS DA crystal, respectively. The absorption spectra are given in Fig. 1(a) and 2(a) for comparison. Figure 1(b) and 2(b) show the REPs for the ν_2 mode, while Fig. 1(c) and 2(c) show those for the ν_1 mode. The circles mark the experimentally determined Raman intensities and the full lines give the results of the least-squares fits of Eq. (18) to the experimental data. The wave number positions of laser excitation are marked by vertical lines. The mean values for the parameters Γ^α and γ obtained from the REPs of all investigated DA crystals are given in Table III. We found considerable variations for both parameters. The main result is, that these variations are strongly related to crystal quality. The values for both γ and Γ^α increase when the crystals show defect structures such as streaks in the transparency. Defect properties play an essential role in DA as well as PDA crystals. Several papers are concerned with defects in DAs and PDAs.⁵¹ Defects also seem to be correlated with the observation of chromism in these substances.^{6,14} The interactions between the molecules and their surroundings were taken into consideration by the introduction of the inhomogeneous broadening, which is characterized by the parameter γ . Defects directly lead to changes of the monomer matrix, which can be regarded as solvent for the polymer chains. Siebrand *et al.*⁴⁹ showed that in solutions not only solvent-induced inhomogeneous but also a solvent-induced homogeneous broadening arises. A strict separation of properties of the ensemble and those of the individual molecules therefore is not possible. The small influence of the defects

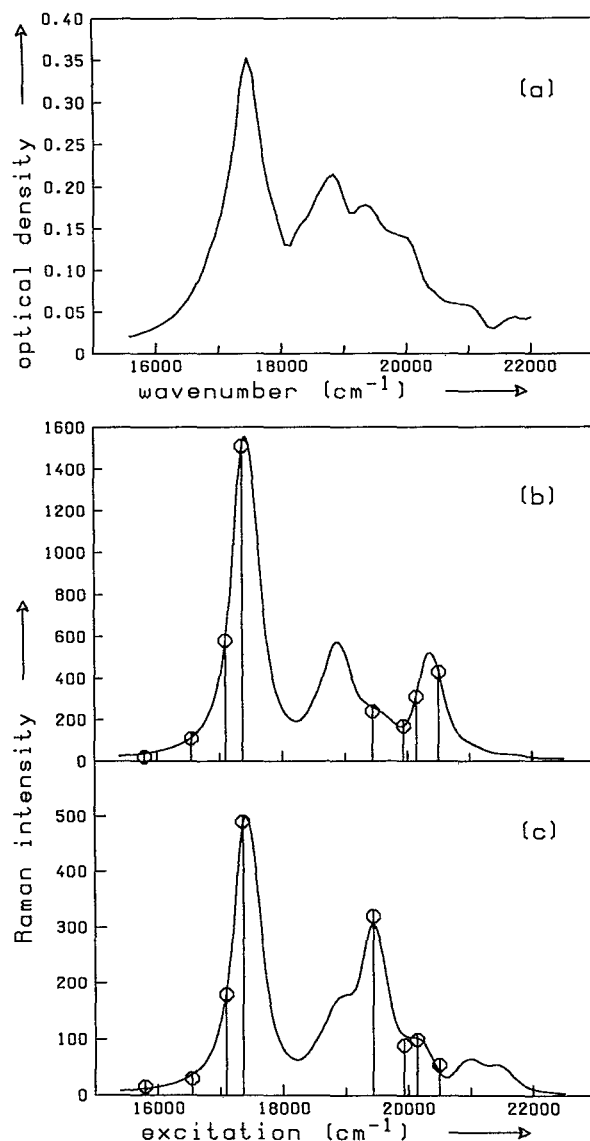


FIG. 1. (a) Absorption spectrum and [(b,c)] resonance Raman excitation profiles (REPs) of an FBS DA crystal, taken at $T = 10$ K, for the ν_2 (b) and the ν_2 mode (c). Solid lines in (b) and (c) are calculated REPs and the circles represent measured Raman intensities. The vertical lines indicate the wave number positions of laser excitation.

on the chain length dependence Γ^B points out that there are different contributions to this homogeneous broadening mechanism, which are not equally influenced by the crystal defects. A further effect of the defects can be seen from the chain length distribution $P(n)$. There is a trend to wider distributions for lower crystal quality.

The examples given in Figs. 1 and 2 were chosen to elucidate these defect properties. The FBS DA crystal contained few visible defects, while the TS/FBS DA crystal exhibited streaks in the transparency, which points to crystal defects. The parameters for the theoretical REPs are given in Table IV. The distribution of chain lengths is additionally shown in Fig. 3, which exhibits the function $P'(n)$ calculated with the parameters for FBS and those for TS/FBS. The

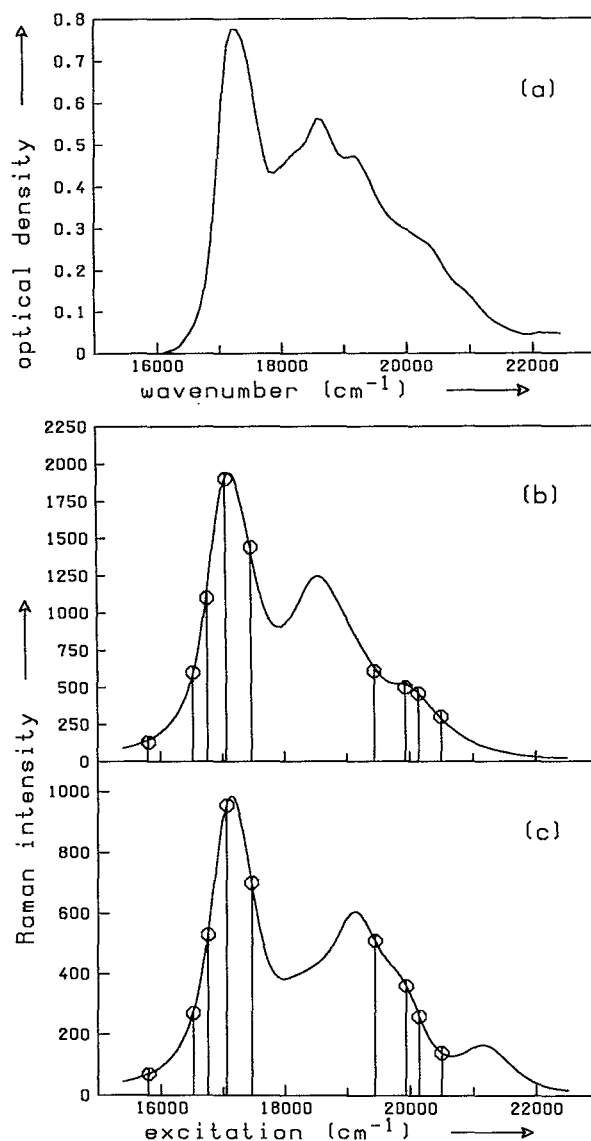


FIG. 2. Same as Fig. 1 except for TS/FBS DA crystals.

distribution is much broader for TS/FBS than for FBS and additionally shifted to larger chain lengths. Such distinct differences are not always observable, but an analogous trend can be observed in most cases. The values of the parameters Γ^a and γ for FBS are smaller than the mean values given in Table II, while those of TS/FBS are larger. The changes of both, the chain length distribution and the homogeneous and inhomogeneous broadening, can also be seen in Figs. 1 and 2. The REPs are much more structured for the DA FBS than for TS/FBS.

To illustrate the effect of the two broadening mechanisms, we calculated REPs using the parameters obtained for the TS/FBS DA crystal. We chose an arbitrary, constant value for $\gamma + \Gamma^a$ (200 cm^{-1}) and varied the ratio of the two parameters. In Fig. 4 these theoretical curves are shown for three ratios: $(\gamma:\Gamma^a) = (100:100)$ (solid line), $(\gamma:\Gamma^a) = (200:0)$ (dash-dotted line), and $(\gamma:\Gamma^a)$

TABLE III. Mean values of the parameters obtained from a least-squares fit to resonance Raman spectra of the three considered types of DA crystals. σ_1 , σ_2 , and σ_{CH_2} are the line widths of the $\text{C}\equiv\text{C}$ -, $\text{C}=\text{C}$ -, and Fermi-resonance mode, respectively. Γ and γ are the homogeneous and inhomogeneous damping constants of the excitation, respectively. The standard deviations for the line width parameters were estimated to be less than 20%. The variations found for the parameters γ and Γ^α were up to 70%. α and β are the constant and chain length dependent part of the parameters, respectively.

DA crystal	Part	σ_1 [cm^{-1}]	σ_2 [cm^{-1}]	σ_{CH_2} [cm^{-1}]	Γ [cm^{-1}]	γ [cm^{-1}]
FBS	α	8	-7	-2	25	150
	β	1130	2520	1200	... ^a	...
TS/FBS	α	7	-4	-1	30	120
	β	810	2190	1010	... ^a	...
TS6 ^b	α	8	-1	1	35	110
	β	590	1450	1070	... ^a	...

^aSee Table II.

^bParameters for $T = 150$ K.

= (0:200) (dashed line). The curves were scaled to be equal at $20\,200\text{ cm}^{-1}$. The variations are appreciable. Inhomogeneous broadening reduces the spectral resolution of the REPs more than homogeneous broadening. This is due to the fact that it does not conserve phase relations and hence does not show structure due to interference.⁴⁹ The vertical lines in Fig. 4 show the wave number positions of the laser lines which have been used for excitation of the resonance Raman spectra. The latter elucidate that it is possible to determine suitable values for γ and Γ .

TS6 DA crystals show deviations in the optical spectra at low temperatures from those of FBS and TS/FBS crystals. Below about 160 K TS6 DA crystals (180 K for PDAs) undergo a phase transition which results in a doubled unit cell containing polymer chains with slightly different structures⁵² (type A and B). The optical absorption splits into two components which have been identified with the two types of polymer chains.⁵³ Similarly several Raman lines, including ν_3 and ν_4 , split into two components while others, such as the ν_1 and ν_2 lines, appear to be unaffected by the phase transition.⁵⁴ In our investigations concerning the absorption spectra of the three DAs¹⁷ mentioned we also calculated the TS6 absorption spectra for $T = 10$ K. From these studies we obtained the FCSPs and the values of Γ^β for both types of

TABLE IV. Values of parameters estimated from the DA spectra in Figs. 1, 2, and 6. The chain length distributions were estimated from the absorption^a and the inhomogeneous (γ) and the constant part of the homogeneous damping (Γ^α) from the resonance Raman excitation profiles. n_0 is the center and Δ the width of the distribution.

DA crystal	n_0	Δ	Γ^α [cm^{-1}]	γ [cm^{-1}]
FBS	11.4	0.06	12	130
TS/FBS	13.9	0.19	53	190
TS6 ^b	11.7	0.22	26	70

^aSee Ref. 17.

^bParameters for $T = 150$ K.

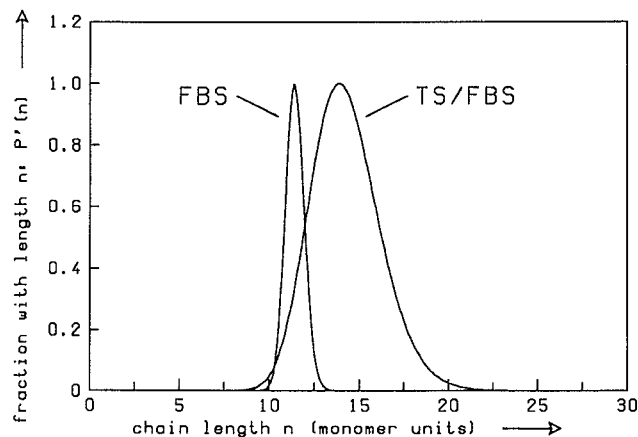


FIG. 3. The function $P'(n)$ [see Eq. (7)] for the parameters n_0 and Δ used in the calculations of the FBS and TS/FBS DA spectra, which are shown in Figs. 1 and 2, respectively. The parameters are listed in Table IV.

polymer chains. These parameters are listed in Table II. For the calculation we assumed a splitting of the high temperature $^1A_g-^1B_u$ transition into two for low temperatures, having different energies. Without further assumptions the model used for the description of the resonance Raman spectra is not able to describe in which way the unsplit Raman lines are related to the different polymer chains. Batchelder *et al.*¹³ performed Franck-Condon calculations to reproduce REPs and absorption spectra of TS6 PDA crystals obtained at $T = 295$ K. With the help of this model they estimated the strength of the coupling between the electronic excited state and the four phonons in the single crystal. This coupling is described by the FCSPs. A comparison between these FCSPs (listed in Table II) and those estimated for the A and B low temperature phases, shows that they are different. The FCSPs for the modes ν_3 and ν_4 show the greatest deviations. This certainly is due to the strong influence of the

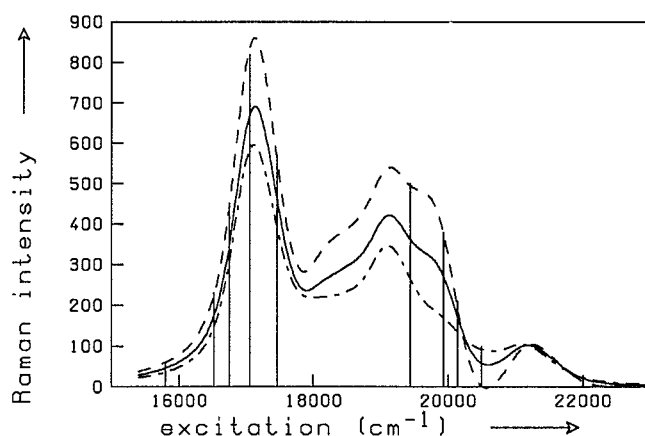


FIG. 4. Influence of the ratio ($\gamma:\Gamma^\alpha$) on the calculated Raman excitation profile. Different parameters for the TS/FBS DA crystal were used: ($\gamma:\Gamma^\alpha$) = (100:100) (solid line), ($\gamma:\Gamma^\alpha$) = (200:0) (dash-dot line), and ($\gamma:\Gamma^\alpha$) = (0:200) (dashed line). The curves were scaled as to coincide at $20\,200\text{ cm}^{-1}$. The vertical lines indicate the wave number positions of the excitation frequencies used in this work.

side group geometry on both modes. This geometry is particularly influenced by the second-order phase transition.⁵⁵ The values of the FCSPs for modes ν_1 and ν_2 obtained for room temperature lie between those obtained for phases *A* and *B* at $T = 10$ K. The room temperature measurements were performed on PDAs, while in our work DAs are investigated. Therefore, it is not certain whether these values are comparable at all. For this reason we took resonance Raman spectra of TS6 DA crystals at $T = 150$ K, which is little below the transition temperature. At this temperature we could not observe any splitting of the absorption lines and nearly no splitting for modes ν_3 and ν_4 . For the theoretical

description of these spectra we therefore used the model given in Sec. II, without any changes. Because of the temperature shift we had to perform a correction of the absorption energies for the higher temperatures, to obtain a suitable chain length dependence. For this purpose we used results published in Ref. 56, which give the dependence of the absorption energies on temperature changes.

We performed several resonance Raman measurements on different TS6 DA crystals for $T = 150$ K. The results shall be introduced guided by an example. Figure 5 exhibits the REPs for the modes ν_1 [Fig. 5(c)] and ν_2 [Fig. 5(b)] of a TS6 DA crystal. In panel (a) of Fig. 5 we show the absorption spectrum. After correction for the higher temperature we were able to fit Eq. (18) to the measured Raman intensities marked as circles in Fig. 5. For this purpose we used the parameters for the *A* and those for the *B* chain (see Table II). The results are shown as dashed lines for the *A*- and as full lines for the *B*-parameters. The *B* curves fit the measured data distinctly better than the *A* curves. This means that the phonons with wave numbers $\tilde{\nu}_1$ and $\tilde{\nu}_2$ can be assigned to *B*-polymer chains for $T = 150$ K. The mean values of the parameters γ and Γ^α obtained for the least-squares fits of all TS6 REPs using FCSPs and Γ^β of *B* type are listed in Table III. Table IV gives the parameters used for the calculations in the example presented in Fig. 5. The results are nearly equivalent to those obtained for FBS and TS/FBS and no further statements can be made.

The previous discussion was concerned with the REPs obtained from the resonance Raman measurements on the considered DAs. As mentioned above the theoretical model introduced in Sec. II should also allow to calculate the shape of the Raman lines. The adaptation of these RLPs is a further test for correct values of the parameters obtained by least-squares fits. By varying the chain length dependence of the line widths and of the wave number positions of modes ν_1 and ν_2 we achieved fairly good agreement between measured and calculated RLPs for all excitation wavelengths. The Fermi resonance enhanced side group mode is described by the line width σ_{CH_2} and the perturbation parameters $W_{\text{CH}_2,2}$ and δ [see Eqs. (11) and (12)]. The mean values obtained

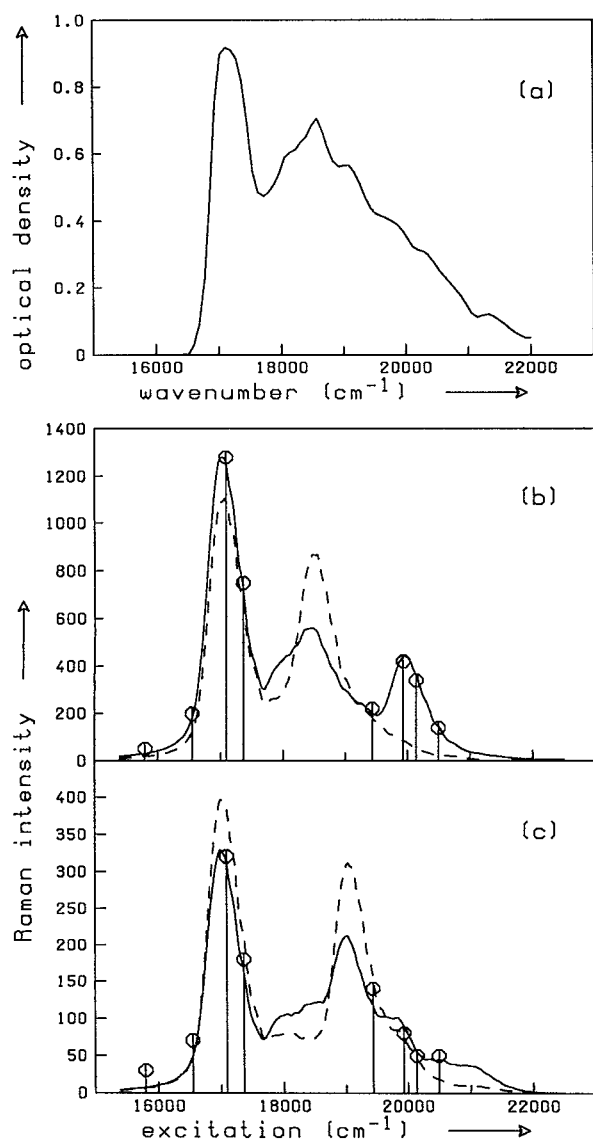


FIG. 5. Absorption spectrum (a) and resonance Raman excitation profiles [(b) and (c)] of a TS6 DA crystal, taken at $T = 150$ K. Panel (b) exhibits the Raman excitation profile for the ν_2 and panel (c) for the ν_1 mode, respectively. The full lines in (b) and (c) are the results of least-squares fits of Eq. (18) to the measured Raman intensities (\circ) using the parameters for the *B* phase. The dashed lines were calculated using the parameters for the *A* phase. The vertical lines indicate the wave number positions of laser excitation.

TABLE V. Mean values of the parameters obtained from a least-squares fit to resonance Raman spectra of the three considered types of DA crystals. $\tilde{\nu}_1$ and $\tilde{\nu}_2$ are the wave numbers for the $\text{C}\equiv\text{C}$ - and the $\text{C}=\text{C}$ -stretching mode, respectively. $W_{\text{CH}_2,2}$ and δ are the parameters, which describe the Fermi resonance [see Eqs. (11) and (12)]. α and β are the constant and chain length dependent part of the parameters, respectively. The standard deviations estimated for the wave number parameters are less than 15% and those for the Fermi parameters less than 10%.

DA crystal	Part	$\tilde{\nu}_1$ [cm ⁻¹]	$\tilde{\nu}_2$ [cm ⁻¹]	$W_{\text{CH}_2,2}$ [cm ⁻¹]	δ [cm ⁻¹]
FBS	α	1985	1451	7	7
	β	530	290	32	-49
TS/FBS	α	2002	1459	7	5
	β	420	200	30	-42
TS6 ^a	α	2010	1462	7	5
	β	350	180	28	-45

^a Parameters for $T = 150$ K.

for the line widths σ are listed in Table III, while those for the wave number positions and Fermi resonance are given in Table V. The standard deviations for these values are all relatively small. The great influence of the substituents on the polymer backbones can be seen from the changes of the σ s and $\tilde{\nu}$ s comparing the DAs FBS, TS/FBS, and TS6. While the parameters for the CH_2 -scissors vibrational mode are nearly unaffected, the chain parameters σ^β and $\tilde{\nu}^\beta$ for modes ν_1 and ν_2 decrease steadily from FBS over TS/FBS to TS6. The best test to control these changes would be to investigate stable oligomers of the different DAs, having a definite length. An elucidation of the primary reaction steps and in-

termediate products succeeded for the DAs FBS,⁵⁷ TS6,³¹ and TS/FBS.⁶ These investigations showed, that it is not possible to produce stable oligomers alone. There are also reactive DA chains of different length present, which show further reaction if exposed to laser light. This reaction is due to a heating as well as to a bleaching process and results among others in stable oligomers. Therefore, a definite resonance Raman spectroscopic investigation of DA oligomers would be very difficult. Investigations of separated chains certainly show deviations due to the missing crystal environment, but can serve for a qualitative comparison. For the compounds $\text{C}_2\text{H}_5\text{OOC}(\text{CH}=\text{CH})_n\text{COOC}_2\text{H}_5$, the frequency of the Raman line at 1600 cm^{-1} decreases steadily from 1643 cm^{-1} ($n=2$) to 1542 cm^{-1} ($n=8$) with increasing chain length.⁴⁴ This decrease is comparable with the one estimated by us for the DA crystals. The reason for the lowering of the chain mode frequencies is the increase of the electron delocalization in conjugated systems with longer chain length.⁵⁸ Differences in the frequencies of the modes ν_1 and ν_2 were also observed for several other PDA molecules.⁹ Also small changes of the substituents lead to relatively great changes of the electronic as well a vibrational properties of these polymers.

As example we present in Fig. 6 RLPs in the considered wave number regions for the excitation wavelengths 488 nm, 567 nm, and 597 nm. The wavelengths were chosen to be in and out of resonance with the ${}^1A_g \rightarrow {}^1B_u$ 0-0 transition showing up in the absorption spectra in Figs. 1(a), 2(a), and 5(a) for FBS, TS/FBS, and TS6, respectively. In panels (a)–(d) of Fig. 6 we display Raman spectra of the FBS crystal, of which absorption spectrum and REPs are given in Fig. 1. Panels (e)–(h) and panels (i)–(l) of Fig. 6 show similar results for TS/FBS and TS6, respectively (compare Figs. 2 and 5 for absorption spectra and REPs, respectively). The upper spectra in each panel are the least-squares fits to the experimental spectra displayed underneath. The calculated RLPs reproduce the measured ones very well. The influence of the distribution of chain lengths can be seen clearly by comparing the RLPs shown for TS/FBS in panels (e)–(h) of Fig. 6. The RLPs shown for FBS and TS6 exhibit qualitatively the same properties. The excitation wavelength chosen for this example is $\lambda_{\text{exc}} = 597\text{ nm}$ [\rightarrow resonance (R)-RLPs], while $\lambda_{\text{exc}} = 488\text{ nm}$ does not coincide with the main 0-0 transition (belonging to chains with $n \approx n_0$). Instead it is on the anti-Stokes side of this transition, giving rise to near resonance (NR)-RLPs. The R-RLPs are more symmetric than the NR-RLPs, which also show larger linewidths. Furthermore, the NR-RLPs are slightly shifted to the anti-Stokes sides with respect to the R-RLPs. Considering the doublet ν_2/ν_{CH} , shown in panels (h) and (f) of Fig. 6, a change of the ratio of the peak intensities of the two lines can be observed. All these properties are reproduced by the theoretical model and are a consequence of different chain length distributions. Excitation with $\lambda_{\text{exc}} = 597\text{ nm}$ yields to a strong enhancement of the intensity of the resonance Raman modes belonging to the chain lengths $n \approx n_0$ resulting in RLPs, which are mainly determined by the lines belonging to only one or two polymer chain lengths. Therefore, the RLPs are relatively symmetric. Exciting at higher

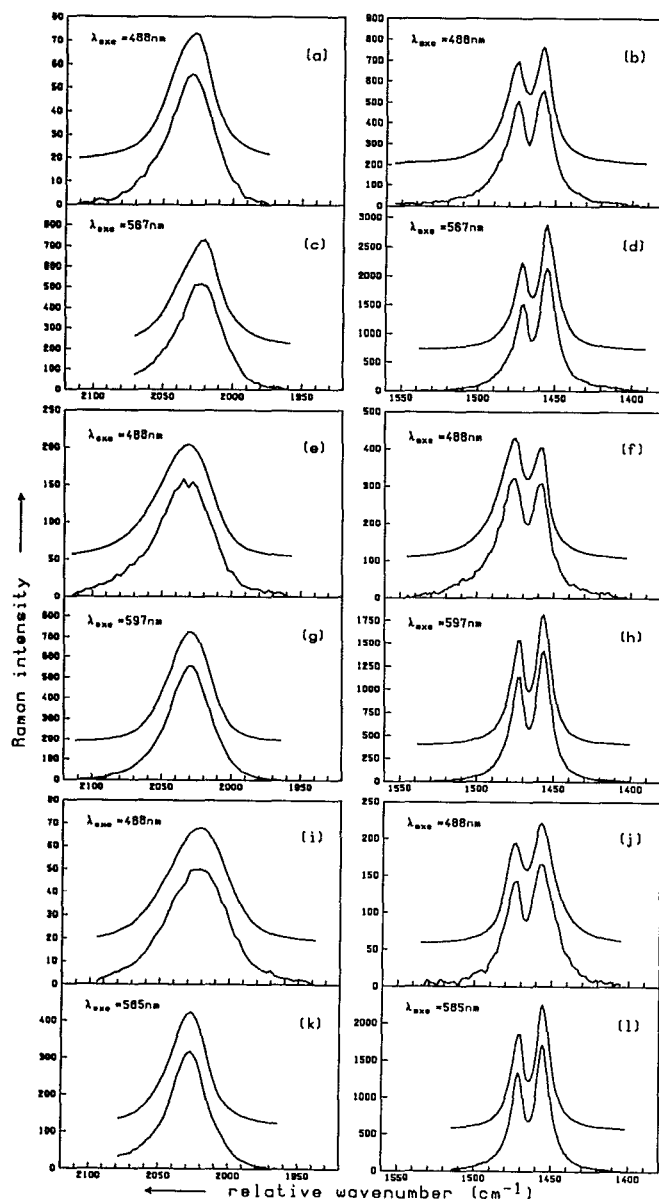


FIG. 6. Resonance Raman spectra obtained for the DA crystals of FBS [(a)–(d), $T = 10\text{ K}$], TS/FBS [(e)–(h), $T = 10\text{ K}$], and TS6 [(i)–(l), $T = 150\text{ K}$]. The lower curves show the measured and the upper ones the fitted Raman line profiles. The excitation wavelengths are labeled for each spectrum. The spectra on the left side show the combination of the ν_2 mode with the Fermi-resonance enhanced ν_{CH} mode.

energies means excitation also of modes belonging to shorter chains. Due to the chain length dependence of the electronic transition matrix elements $[\mu_x]_{eg}^0$ also longer chain lengths remarkably contribute to the NR-RLPs. A simple evaluation of this dependence by the field-emission microscopy free electron model (FEM) theory applied by Kuhn⁵⁹ results in the following: The oscillator strength of the HOMO–LUMO transition in this theory is given by

$$f_{1,1} = \frac{2m_e}{3\hbar^2} \Delta E_{1,1} [\mu_x]_{1,1}^2 = \frac{128}{3\pi^2} \frac{n^2(4n+2)^2}{(4n+1)^3}, \quad (19)$$

where m_e is the electron mass. The energy $\Delta E_{1,1}$ in FEM is given by

$$\Delta E_{1,1} = \frac{\hbar^2 \pi^2}{2m_e} \frac{4n+1}{L^2}, \quad (20)$$

where L is the length of the conjugated π -electron system. Taking into consideration that $L \propto n$ results in $[\mu_x]_{1,1}^4 \propto n^4$. The combination of all these contributions gives rise to unsymmetrical Raman profiles as well as to anti-Stokes shifts of the NR-RLPs. The enhancement also of shorter chains additionally results in the change of the intensity ratio for the Fermi-resonance doublet. The parameter δ (see Table V) changes sign if n becomes smaller than 7–9 monomer units. This means that the unperturbed wave numbers $\tilde{\nu}_2$ and $\tilde{\nu}_{CH_2}$ are nearly degenerate for a distinct chain length. Similar results were reported for investigations of PDA crystals, where variable stress resulted in comparable changes of the intensity ratio.⁴⁷ The n dependence of the electronic transition matrix elements prevents more distinct changes of the intensity ratio.

IV. CONCLUSION

Freshly grown diacetylene single crystals of the DAs FBS, TS/FBS, and TS6 contain few polymer chains, which are embedded in the monomer matrix. These chains are short and their lengths are not uniform but can be described by a distribution function similar to a log-normal function. The resonance Raman spectra of the DA crystals under study show Raman excitation (REPs) and Raman line profiles (RLPs), which can be only explained satisfactorily by taking into account a chain length dependence of several electronic and vibrational properties. The latter is taken care of by a Franck–Condon model, which describes the REPs as well as the RLPs. Applying the crude Born–Oppenheimer approximation the pure electronic transition matrix elements as well as the energies of the transitions can be estimated by means of LCAO MO calculations in the Hückel approach. The matrix elements of the Franck–Condon integrals are calculated assuming harmonic potentials with same curvature for ground and excited states. By using a simple recurrence relation these integrals can be evaluated as functions of the Franck–Condon vibrational shift parameters (FCSPs), which in earlier studies were found to be independent of chain length. The chain length dependence of the other parameters have been obtained mainly from comparisons with results from similar conjugated systems. It has been shown that the assumption of inhomogeneous broadening of the energies of the excited states plays an important

role. Inhomogeneous broadening has been taken into account in the expression for the Raman intensity by means of a distribution of excitation energies.

The resulting expression for the resonance Raman intensity is used to fit the REPs as well as the RLPs of several series of Raman spectra obtained from each type of DA. Particularly, the modes ν_1 and ν_2 have been considered in detail. The ν_2 Raman line is accompanied by a Fermi resonance enhanced side group mode. The measured Raman intensities can be very well reproduced by the theoretical model. The experimental and theoretical studies allow to obtain information mainly concerning the FCSPs and the damping parameters in the electronic resonance part of the Raman intensity. An interesting result from these computations is that defects of the DA crystals strongly influence both, the constant part of the homogeneous and the inhomogeneous damping. This results in considerable changes of the REPs obtained for the DA crystals under investigation. The reason for this is a mutual affecting of ensemble and intramolecular properties due to the perturbation by the defects. Calculations for TS6 DA resonance Raman spectra obtained at temperature slightly below the second-order phase transition also yields interesting results. It could be shown that mainly one of the two types of polymer chains resulting from the phase transition seems to determine the REPs of the considered Raman modes.

The measured RLPs are also reproduced by the theoretical model. It could be shown that the changes in line positions as well as line shapes are due to the distribution of chain lengths in the DA crystals. The variations of the ratio of the intensity of mode ν_2 and the one of the Fermi-resonance enhanced CH_2 -scissors vibration for different Raman excitations could also be explained by the enhancement of modes belonging to chains of different lengths. The values obtained for the parameters belonging to the different types of DAs proof a strong influence of the substituents on the properties of the delocalized π -electron system of the polymer backbones.

The distribution of the lengths of conjugation as well as the influence of crystal defects seem to be essential for the description of all DA and PDA crystals. The occurrence of different kinds of chromism in many types of DAs is due to these properties. A further investigation especially of defect induced changes in DA and PDA crystals would help to gain a more deeper understanding of many of their properties.

ACKNOWLEDGMENTS

We wish to thank Professor Markus Schwoerer, University of Bayreuth, for making the DA crystals available to us. Some of the absorption measurements were performed in his laboratory. We are very grateful to Mrs. Irene Müller for growing the excellent crystals. One of us (A.M.) thanks the Stiftung Volkswagenwerk and the Fonds der Chemischen Industrie for a postgraduate scholarship. Financial support from the Fonds der Chemischen Industrie e.V. and the Deutsche Forschungsgemeinschaft (SFB) 347, Projekt C-2) is highly acknowledged.

- ¹G. J. Blanchard and J. P. Heritage, *J. Chem. Phys.* **93**, 4377 (1990).
- ²G. M. Carter, Y. J. Chen, and S. K. Tripathy, *Appl. Phys. Lett.* **43**, 891 (1983).
- ³R. R. Chance, M. L. Shand, C. Hogg, and R. Silbey, *Phys. Rev.* **B22**, 3540 (1980).
- ⁴G. Wegner, *Z. Naturforsch. B* **24**, 824 (1969).
- ⁵G. J. Exarhos, W. M. Risen, Jr., and R. H. Baughman, *J. Am. Chem. Soc.* **98**, 481 (1976).
- ⁶H.-D. Bauer, A. Materny, I. Müller, and M. Schwoerer, *Mol. Cryst. Liq. Cryst.* **200**, 205 (1991).
- ⁷C. J. Eckhardt, H. Mueller, J. Tylicki, and R. R. Chance, *J. Chem. Phys.* **65**, 4311 (1976).
- ⁸M. R. Philpott, *J. Chem. Phys.* **63**, 485 (1975).
- ⁹R. H. Baughman, J. D. Witt, and K. C. Yee, *J. Chem. Phys.* **60**, 4755 (1974).
- ¹⁰D. N. Batchelder and D. Bloor, in *Advances in Infrared and Raman Spectroscopy*, edited by R. J. H. Clark and R. E. Hester (Wiley, New York, 1984), Vol. 11, Chap. 4.
- ¹¹L. X. Zheng, R. E. Benner, Z. V. Vardeny, and G. L. Baker, *Synth. Met.* **41-43**, 235 (1991).
- ¹²D. Bloor, F. H. Preston, D. J. Ando, and D. N. Batchelder, in *Structural Studies of Macromolecules by Spectroscopic Methods*, edited by K. J. Ivin (Wiley, Chichester, 1976), p. 91.
- ¹³D. N. Batchelder and D. Bloor, *J. Phys. C*, **15**, 3005 (1982).
- ¹⁴A. Materny, M. Leuchs, T. Michelis, K. Schaschek, and W. Kiefer, *J. Raman Spectrosc.* **23**, 99 (1992); A. Materny and W. Kiefer, *Macromolecules* (in press); A. Materny, M. Schwoerer, and W. Kiefer, *J. Chem. Phys.* (in press).
- ¹⁵A. Materny, M. Schwoerer, and W. Kiefer, in *Proceedings of the XIIth International Conference on Raman Spectroscopy*, edited by J. R. Durig and J. F. Sullivan (Wiley, Chichester, 1990), p. 742.
- ¹⁶M. Ganz, W. Kiefer, A. Materny, and P. Vogt, *J. Mol. Struct.* **266**, 115 (1992).
- ¹⁷A. Materny and W. Kiefer, *Phys. Rev. B*, in press and *J. Raman Spectrosc.* (submitted).
- ¹⁸G. Wegner, in *Molecular Metals*, edited by W. E. Hatfield (Plenum, New York, 1979).
- ¹⁹V. Enkelmann, *Makromol. Chem.* **184**, 1945 (1983).
- ²⁰P. Strohmriegel, *Makromol. Chem., Rapid Commun.* **8**, 437 (1987).
- ²¹M. Bertault, L. Toupet, J. Canceill, and A. Collet, *Makromol. Chem., Rapid Commun.* **8**, 443 (1987).
- ²²H. A. Kramers and W. Heisenberg, *Z. Phys.* **31**, 681 (1925); P. A. M. Dirac, *Proc. R. Soc. London, Ser. A* **114**, 710 (1927).
- ²³See, for example, R. J. H. Clark and B. Stewart, *J. Am. Chem. Soc.* **103**, 6593 (1981).
- ²⁴G. Placzek, in *Handbuch der Radiologie*, edited by E. Marx (Akademischer Verlag, Leipzig, 1934), Vol. VI, Part II, p. 209.
- ²⁵A. C. Albrecht, *J. Chem. Phys.* **34**, 1476 (1961).
- ²⁶D. N. Batchelder, in *Polydiacetylenes*, edited by D. Bloor and R. R. Chance, NATO ASI Series (Nijhoff, Dordrecht, 1985), Vol. E 102, p. 187.
- ²⁷W. F. Lewis and D. N. Batchelder, *Chem. Phys. Lett.* **60**, 232 (1979).
- ²⁸C. Manneback, *Physica* **17**, 1001 (1951).
- ²⁹R. J. H. Clark and T. J. Dines, *Angew. Chem.* **98**, 131 (1986).
- ³⁰F. Inagaki, M. Tasumi, and T. Miyazawa, *J. Mol. Spectrosc.* **50**, 286 (1974).
- ³¹H. Sixl, in *Polydiacetylenes*, edited by H. J. Cantow, *Advances in Polymer Science* (Springer, Berlin, 1984), Vol. 63, p. 49.
- ³²R. Warta, Ph. D. thesis, University of Stuttgart, 1989 (unpublished).
- ³³M. F. Granville, B. E. Kohler, and J. Bannion Snow, *J. Chem. Phys.* **75**, 3765 (1981).
- ³⁴L. Rimai, M. E. Heyde, and D. Gill, *J. Am. Chem. Soc.* **95**, 4493 (1973).
- ³⁵H. Kuzmany, P. Knoll, in *Electronic Properties of Polymers and Related Compounds*, edited by H. Kuzmany, M. Mehring, and S. Roth (Springer, Berlin, 1985), p. 114.
- ³⁶G. P. Brivio and E. Mulazzi, *Chem. Phys. Lett.* **95**, 555 (1983).
- ³⁷H. E. Schaffer, R. R. Chance, R. J. Silbey, K. Knoll, and R. R. Schrock, *J. Chem. Phys.* **94**, 4161 (1991).
- ³⁸R. H. Baughman and R. R. Chance, *J. Polym. Sci. Polym. Phys. Ed.* **14**, 2037 (1976).
- ³⁹P. A. Albouy, J. N. Patillon, and J. P. Pouget, in *Polydiacetylenes*, edited by D. Bloor and R. R. Chance, NATO ASI Series (Nijhoff, Dordrecht, 1985), Vol. E 102, p. 67.
- ⁴⁰H. Eckhardt, D. S. Boudreaux, and R. R. Chance, *J. Chem. Phys.* **85**, 4116 (1986).
- ⁴¹Y. Tomioka, N. Tanaka, and S. Imazeki, *J. Chem. Phys.* **91**, 5694 (1989).
- ⁴²T. A. Albright, J. K. Burdett, and M.-H. Whangbo, *Orbital Interactions in Chemistry* (Wiley, New York, 1985).
- ⁴³J. C. Slater, *Phys. Rev.* **36**, 57 (1930).
- ⁴⁴A. J. Melveger and R. H. Baughman, *J. Polym. Sci. Polym. Phys. Ed.* **11**, 603 (1973).
- ⁴⁵H. Gross, Ph. D. thesis, University of Stuttgart, 1983.
- ⁴⁶H. Kuzmany, *Pure Appl. Chem.* **57**, 235 (1985).
- ⁴⁷D. N. Batchelder and D. J. Bloor, *J. Polym. Sci. Polym. Phys. Ed.* **17**, 569 (1979); D. Bloor, D. J. Ando, C. L. Hubble, and R. L. Williams, *ibid.* **18**, 779 (1980).
- ⁴⁸G. Herzberg, *Molecular Spectra and Molecular Structure* (Nostrand, New York, 1954), Vol. II.
- ⁴⁹W. Siebrand and M. Zgierski, *J. Chem. Phys.* **71**, 3561 (1979); W. Siebrand and M. Zgierski, *J. Phys. Chem.* **86**, 4718 (1982).
- ⁵⁰D. W. Marquardt, *J. Soc. Ind. Appl. Math.* **11**, 431 (1963); W. H. Press, B. P. Flannery, S. A. Teukolsky, and W. T. Vetterling, *Numerical Recipes in C* (Cambridge University, Cambridge, 1988), Chap. 14.
- ⁵¹D. Bloor, D. N. Batchelder, and F. H. Preston, *Phys. Stat. Sol. (a)* **40**, 279 (1977); M. Dudley, J. N. Sherwood, D. J. Ando, and D. Bloor, in *Polydiacetylenes*, edited by D. Bloor and R. R. Chance, NATO ASI Series (Nijhoff, Dordrecht, 1985), Vol. E 102, p. 87.
- ⁵²V. Enkelmann, *Acta Crystallogr.* **333**, 2842 (1977).
- ⁵³D. Bloor and F. H. Preston, *Phys. Status Solidi (a)* **39**, 607 (1977).
- ⁵⁴D. N. Batchelder and D. Bloor, *Chem. Phys. Lett.* **38**, 37 (1976).
- ⁵⁵R. L. Williams, D. Bloor, D. N. Batchelder, M. B. Hursthouse, and W. B. Daniels, *Faraday Discuss. Chem. Soc.* **69**, 49 (1980).
- ⁵⁶A. C. Cottle, W. F. Lewis, and D. N. Batchelder, *J. Phys. C*, **11**, 605 (1978); D. Bloor and C. L. Hubble, *Chem. Phys. Lett.* **78**, 89 (1978).
- ⁵⁷R. Warta and H. Sixl, *J. Chem. Phys.* **88**, 95 (1988).
- ⁵⁸R. M. Gavin, Jr. and S. A. Rice, *J. Chem. Phys.* **55**, 2675 (1971).
- ⁵⁹H. Kuhn, *Helv. Chim. Acta* **34**, 1308 (1951).